

## High-Speed Microcontact Printing

Jo A. Helmuth,<sup>‡</sup> Heinz Schmid,<sup>\*†</sup> Richard Stutz,<sup>†</sup> Andreas Stemmer,<sup>‡</sup> and Heiko Wolf<sup>†</sup>  
Nanotechnology Group, ETH Zurich, CH-8092 Zurich, Switzerland, and Zurich Research Laboratory,  
IBM Research GmbH, 8803 Rüschlikon, Switzerland

Received April 10, 2006; E-mail: sih@zurich.ibm.com

We report on microcontact printing ( $\mu$ CP) with stamp–substrate contact times of 1 ms—three orders of magnitude shorter than typical values of previous studies. High-speed  $\mu$ CP enables a significant process speed-up, improves uniformity and reproducibility of the printed monolayer pattern, and provides insight into the dynamics of printing.

$\mu$ CP is a method to chemically pattern surfaces.<sup>1</sup> A widely used application is the printing of alkanethiols (ink) on noble-metal surfaces, on which they form a self-assembled monolayer (SAM) that can serve as a resist for a selective etch process.<sup>2</sup> Molecules are diffusively transported from the bulk of a structured elastomeric stamp to a substrate upon conformal contact.<sup>3</sup>  $\mu$ CP of a SAM that is free of defects and of high contrast while maintaining good pattern fidelity leads to conflicting parameter adjustments. This difficulty originates from the typically varying dimensions and fill-factors of simultaneously printed patterns.<sup>4</sup> The higher per area amount of ink available for features with a low fill-factor (Figure 1A) will cause an increased flux of molecules to the interface, leading to a laterally nonuniform ink concentration at the stamp–substrate interface and pattern blurring due to lateral diffusion of the ink on the substrate. A strategy to avoid lateral spreading is the use of low diffusion ink molecules.<sup>5</sup> Pattern-dependent ink delivery will be further increased when the stamp is used for subsequent prints. After printing, the ink concentration in the stamp is space- and time-dependent. Defined printing conditions for multiple prints can only be ensured by re-inking or sufficiently long waiting times between prints for equilibration. We show that, by implementing printing conditions that differ drastically from those of previous studies, the depletion layer<sup>6</sup> can be confined to the protrusions (Figure 1B) and print quality becomes independent of the pattern density, even when diffusive inks are used. Numerical diffusion simulations predict that the amount of molecules required to form a monolayer on the surface can be supplied from a 1  $\mu$ m high protrusion in a few milliseconds at a hexadecanethiol (HDT) ink concentration that is substantially below the ink solubility limit of the stamp material and low enough to avoid geometrical distortion of the stamp due to ink-induced swelling. We assume that SAM formation is not a reaction-limited process at that time scale.<sup>7</sup>

Automated positioning, printing, and retraction of the stamp on the substrate are realized with a long-expansion closed-loop piezoelectric actuator mounted on a motorized two-axis stage. An optical system in the stamp holder allows visual observation of the contact. Stamps are made from 100  $\mu$ m thick PDMS, with the smallest features being lines and spaces having a width and height of 1  $\mu$ m, respectively. Effective contact times and their deviation from programmed values were evaluated using a high-speed camera. Lateral variations of the contact time due to a nonflat stamp surface and sealing of air bubbles are below 0.5 ms (Figure 2A,B). The high-speed recordings also reveal the influence of the stamp pattern

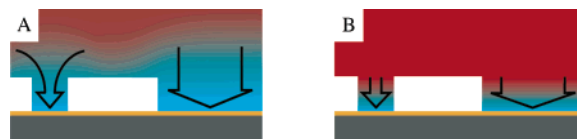


**Figure 1.** Schematic comparison of ink concentrations in stamps after printing. (A) Low ink concentrations and long printing times result in a depletion layer (blue) that extends beyond the protrusions. (B) Fast printing using high ink concentrations leads to a narrow depletion layer. As a result, the ink flux is independent of the stamp pattern.

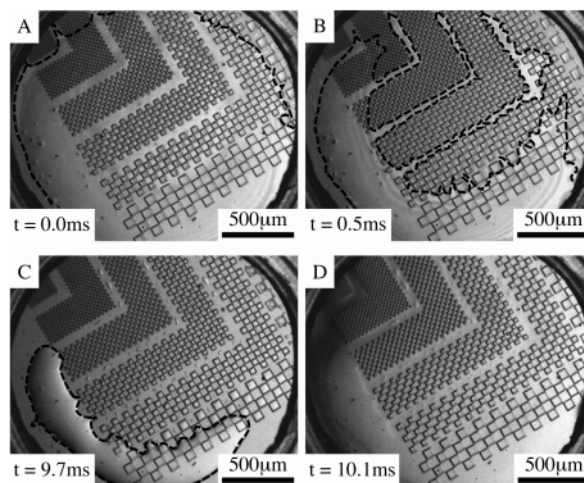


**Figure 2.** High-speed records showing the contact and separation dynamics of a stamp and substrate during a 10 ms print. (A) The contact front (dashed line) spreads from the periphery along the structured areas of the stamp, and (B) broad contact is achieved within 0.5 ms. (C) An air bubble remains sealed owing to the nonperfect planarity of the stamp. (D) Within 0.4 ms, separation is complete.

on contact formation: patterned areas preferentially contact first. We suggest that the recessed areas serve as a buffer volume for trapped air. In addition, the increased surface area enhances the dissolution of trapped air in the stamp. The time scale of these two effects establishes a practical limit of high-speed  $\mu$ CP. Within 0.4 ms, the stamp is separated from the substrate (Figure 2C,D). This demonstrates that a contact time with millisecond accuracy is possible with the current setup and stamp geometry. The fast contact time is further verified by electrical contact measurements using metallized stamps and substrates.

We performed a series of prints using HDT as ink in which the substrates are prepared by evaporating 1 nm Ti followed by 15 nm Au on Si wafers. Stamps are equilibrated on PDMS inkpads for several days to guarantee a homogeneous ink concentration.<sup>8</sup> The ink is supplied to the pads by distributing a drop of pure HDT between two slabs of PDMS. The resulting concentration is measured gravimetrically. Prints are developed by etching in a 0.1 M aqueous KCN solution at pH 12 for 5 min.

<sup>‡</sup> ETH Zurich.

<sup>†</sup> IBM Zurich Research Laboratory.

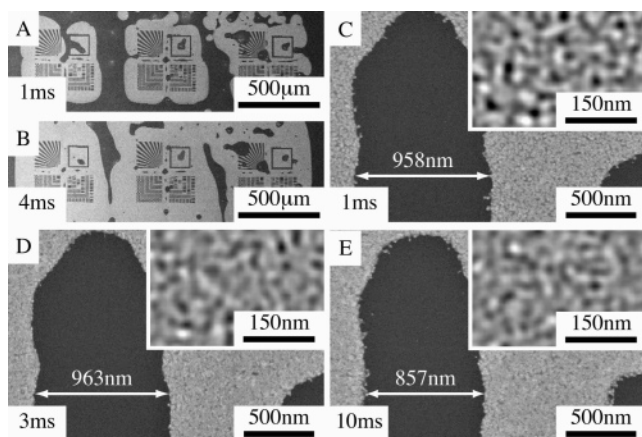


**Figure 3.** SEM images of high-speed-printed and etched Au films (bright). The concentration of HDT in the stamp was 16.6 mM; print times are indicated. (A) Contact is simultaneously established in less than 1 ms on the structured areas and (B) subsequently spreads to the unstructured areas within 3 ms. (C–E): High-resolution images showing the influence of the print time on the etched pattern. Insets are images with increased contrast to visualize the defects. The prints correspond to the same location on the stamp. In (C), the gold layer has small defects, whereas in (D), perfect protection has been achieved. (E) Surface diffusion of HDT is apparent.

In Figure 3, SEM micrographs of printed and subsequently etched Au layers are shown. A series of six prints with increasing print times was carried out using the same stamp for each print. The concentration profile in the stamp was equilibrated by waiting periods of 10 s to guarantee uniform inking for the lowest ink concentration used. Printed and etched samples from a control series with constant print time show no decrease of quality in the first eight prints. Numerical diffusion simulations confirm that the concentration profile is quickly equilibrated and that depletion effects are thus negligible. Figure 3A shows that the contact forms instantaneously on the patterned area, from which it spreads over the unstructured area (Figure 3B). This observation is in very good agreement with the optical contact measurements. The quality of the prints was evaluated using high-resolution images of the etched Au layer. A 1 ms long print using a concentration of 16.6 mM HDT in the stamp results in a Au layer with small point defects (Figure 3C), which indicates that SAM formation was incomplete. In excellent agreement with the numerical simulation, a print time of 3 ms yields a defect-free Au layer (Figure 3D). A further increase of the print time will not yield better etch protection, but affects the reproduction of the patterns negatively because of lateral surface diffusion of the ink (Figure 3E).<sup>4</sup> Loss of contrast due to vapor-phase diffusion becomes first apparent for print times above 30 ms. The high-speed prints show a uniform protection that is independent of the pattern fill-factor, in accordance with the expected narrow depletion layer. On the basis of simulations and experiments (see Table 1 in Supporting Information), we finally compiled a semiquantitative graph to summarize the limits of the process window for high-speed  $\mu$ CP (Figure 4). Printing conditions of standard  $\mu$ CP are indicated, but a quantitative comparison is difficult due to the different inking methods. We conclude that within milliseconds a sufficient amount of HDT can be delivered to the Au substrate to form a protective SAM.

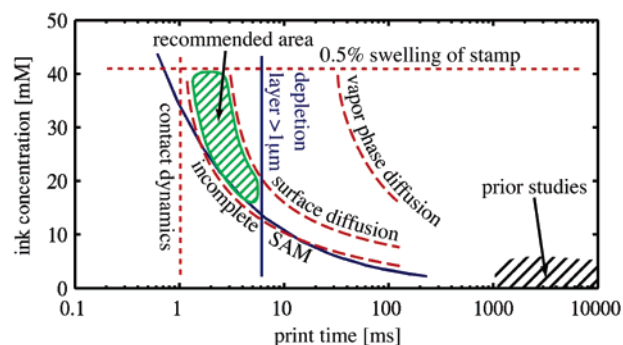


**Figure 4.** Semiquantitative graph illustrating the process window of high-speed  $\mu$ CP. The recommended parameter space is confined by the limits of contact dynamics, the distortion of the stamp due to ink-induced swelling (red dotted lines), the condition for complete SAM formation (blue solid line, simulation; red dashed line, experiment), and surface diffusion, whereas vapor-phase diffusion is not a limiting factor (red dashed lines). Fill-factor-independent ink flux is possible on the left side of the vertical blue line (simulation for 1  $\mu$ m thick depletion layer<sup>6</sup>).

The experimental results are in good agreement with the prediction from a numerical simulation that assumes a non-reaction-limited process. In contrast to standard  $\mu$ CP, good protection and accurate pattern reproducibility were observed independently of the feature density. Finally, mechanics and aerodynamics have been identified as limiting factors for high-speed  $\mu$ CP.

**Acknowledgment.** H.S. and H.W. thank W. Riess for his continuous support. The partial support of the State Secretariat for Education and Research (SER) in the framework of the EC-funded project NaPa (Contract No. NMP4-CT-2003-500120) is gratefully acknowledged.

**Supporting Information Available:** Experimental methods and the setup, stamp fabrication, electrical measurements, and additional experimental results. This material is available free of charge via the Internet at <http://pubs.acs.org>.

## References

- (1) (a) Kumar, A.; Whitesides, G. M. *Appl. Phys. Lett.* **1993**, *63*, 2002–2004. (b) Xia, Y.; Whitesides, G. M. *Annu. Rev. Mater. Sci.* **1998**, *28*, 153–184.
- (2) (a) Bain, C. D.; Troughton, E. B.; Tao, Y.-T.; Evall, J.; Whitesides, G. M.; Nuzzo, R. G. *J. Am. Chem. Soc.* **1989**, *111*, 321–335. (b) Chidsey, C. E. D.; Loiacono, D. N. *Langmuir* **1990**, *6*, 682–691. (c) Xia, Y.; Zhao, X.-M.; Whitesides, G. M. *Microelectron. Eng.* **1996**, *32*, 255–268. (d) Larsen, N. B.; Biebuyck, H.; Delamarche, E.; Michel, B. *J. Am. Chem. Soc.* **1997**, *119*, 3017–3026.
- (3) Bietsch, A.; Michel, B. *J. Appl. Phys.* **2000**, *88*, 4310–4318.
- (4) Delamarche, E.; Schmid, H.; Bietsch, A.; Larsen, N. B.; Rothuizen, H.; Michel, B.; Biebuyck, H. A. *J. Phys. Chem. B* **1998**, *102*, 3324–3334.
- (5) (a) Liebau, M.; Huskens, J.; Reinhoudt, D. N. *Adv. Funct. Mater.* **2001**, *11*, 147–150. (b) Li, H.; Kang, D.-J.; Blamire, M. G.; Huck, W. T. S. *Nano Lett.* **2002**, *2*, 347–349.
- (6) The depletion layer is defined as the volume from which 95% of the ink is delivered to the substrate. Note: This definition does not necessarily assume a full monolayer coverage.
- (7) (a) Balmer, T. E.; Schmid, H.; Stutz, R.; Delamarche, E.; Michel, B.; Spencer, N.; Wolf, H. *Langmuir* **2005**, *21*, 622–632. (b) Kraus, T.; Stutz, R.; Balmer, T. E.; Schmid, H.; Malaquin, L.; Spencer, N. D.; Wolf, H. *Langmuir* **2005**, *21*, 7796–7804.
- (8) Libiouille, L.; Bietsch, A.; Schmid, H.; Michel, B.; Delamarche, E. *Langmuir* **1999**, *15*, 300–304.

JA062461B